

# A Decomposition Approach to Characterizing Feasibility in Acyclic Multi-Unit Processes<sup>\*</sup>

Max Mowbray<sup>\*</sup> Cleo Kontoravdi<sup>\*</sup> Nilay Shah<sup>\*</sup>  
Benoît Chachuat<sup>\*</sup>

<sup>\*</sup> *The Sargent Centre for Process Systems Engineering, Department of  
Chemical Engineering, Imperial College London, London SW7 2AZ,  
United Kingdom*

---

**Abstract:** The ability to certify feasibility in process design and process operations is crucial in many applications. This includes quality-by-design in pharmaceutical manufacturing, where a key element is the characterization of the design space to better understand the links between materials, processes and products. Sampling-based approaches are versatile but they are cursed by dimensionality, which currently limits their application to problems in a few process variables only. We propose a decomposition approach that enables feasibility characterization for nominal settings of uncertain parameters in acyclic multi-unit processes by sampling. Our methodology leverages problem structure to decompose unit-wise, and deploys surrogate models to couple the resultant subproblems. We demonstrate it on a serial, batch chemical reactor network. In future research, we will extend this framework to cyclic multi-unit processes and the presence of parameter uncertainty.

*Keywords:* Process design, Nested sampling, Quality-by-design, Design space, Network structure, Machine learning

---

## 1. INTRODUCTION

The process systems engineering (PSE) community have been developing a wide range of computational tools to aid in the design and operation of (bio)chemical process systems. The incentives for developing efficient frameworks for these decision problems have been reinforced by drives for sustainability and quality by design (QbD), the latter of which is specific to the pharmaceutical industry. The QbD principles leverage model-based decision tools to demonstrate that a drug manufacturing process is capable of consistently meeting targets on key performance indicators, such as product purity, and provides a framework for a pharmaceutical company to gain regulatory approval (Yu et al., 2014). A key part of the QbD philosophy is quantification of the design space (DS) associated with a manufacturing process (von Stosch et al., 2020). The DS describes the set of critical process parameters (CPP) and material attributes that enable satisfaction of given critical quality attributes (CQA) imposed on products. Naturally, the concept of DS extends beyond the pharmaceutical industry to identify the feasible space (FS) of any production process.

A popular approach attempts to inscribe a parameterized shape with maximum volume within the FS, which can be

mathematically formulated as a flexibility index problem without recourse (Swaney and Grossmann, 1985; Zhao et al., 2022b). Common shapes are boxes and ellipsoids, the former of which is the description required in current pharmaceutical regulatory approval processes (von Stosch et al., 2020). A drawback with this approach is that a simple shape may not provide a good approximation of the feasible region and thus introduce significant conservatism. Additionally, the resultant problems formulate as multi-level or semi-infinite mathematical programs, which are challenging to solve to global optimality for general process models (Harwood and Barton, 2017).

As a result, there has been interest in solution methods that can handle complexity or nonconvexity in the FS, while retaining computational tractability. This is reflected by the development of sampling approaches to characterizing feasibility, which provide a potential solution owing to their versatility and nonintrusive nature. They discretize the process variable space and return a set of samples that satisfy all of the feasibility constraints. For example, Kucherenko et al. (2020) proposed an adaptive sampling framework based on surrogate modelling of a process's feasible region. The surrogate model provides an acceptance-rejection mechanism that reduces evaluation of the underlying process model and enables a two-orders of magnitude speed up relative to naive sampling in case study. Zhao et al. (2022a) presented a framework based on adaptive sampling and use of smooth surrogate models to approximate the feasible region's boundary by means of a Kreisselmeier–Steinhauser (KS) constraint aggregation function. Within the spirit of adaptive sampling, Kusumo

---

<sup>\*</sup> This work is co-funded by Eli Lilly & Company through the Pharmaceutical Systems Engineering Lab (PharmaSEL) and by the Engineering and Physical Sciences Research Council (EPSRC) as part of its Prosperity Partnership Programme under grant EP/T518207/1. Correspondence should be directed to Benoît Chachuat: b.chachuat@imperial.ac.uk

et al. (2019) proposed methodology to characterize probabilistic feasibility by taking inspiration from nested sampling, an algorithm typically used within the context of Bayesian estimation. More recently, sampling strategies have also been applied to flexibility problems, which are considered an extension of feasibility that accounts for the action of recourse in enlargement of the feasible region, as demonstrated in the contribution of Geremia et al. (2024). Another example is provided by Kudva et al. (2024), who proposed a Bayesian optimization algorithm to handle the case where one does not have a model of the constraints to satisfy readily available, or the case that model evaluation is particularly expensive.

It is worth noting that the use of sampling remains challenged by the curse of dimensionality, which can render these schemes expensive for FS in few process variables. This is of relevance to multi-unit operations. In this problem setting, one is interested in characterizing the joint FS of multiple units where there exists operational dependency. Feasibility of processing networks has been considered previously, but to the authors' knowledge, these approaches proceed via solution to mathematical programs only (Samsatli et al., 1999).

In this paper, we present a sampling-based methodology to approach multi-unit feasibility, by leveraging process structure and decomposition, and deploying surrogate models to couple the resultant subproblems. We focus on acyclic multi-unit processes and nominal feasibility by neglecting modeling uncertainties. Section 2 provides background on nested sampling, which is the adaptive sampling algorithm of choice. Next, the methodology is detailed in Section 3 and demonstrated with the case study of a batch reactor network in Section 4.

## 2. BACKGROUND

Nested sampling is an adaptive sampling method conventionally used for evidence approximation in Bayesian parameter estimation (Skilling, 2006). It also finds applications in (nominal or probabilistic) feasibility characterization (Kusumo et al., 2019), as well as in set-membership estimation (Paulen et al., 2020). For example, one may wish to characterize the following set:

$$\Theta := \{\boldsymbol{\theta} \in \mathbb{R}^{n_\theta} \mid \mathbf{G}(\boldsymbol{\theta}) \leq \mathbf{0}\} \quad (1)$$

where  $\mathbf{G} : \mathbb{R}^{n_\theta} \rightarrow \mathbb{R}^{n_g}$  describes a system of inequality constraints. For application of nested sampling, alternative descriptions of the inequality constraints that provide an analogue to the likelihood function are required. A simple example is provided by:

$$\Theta = \{\boldsymbol{\theta} \in \mathbb{R}^{n_\theta} \mid \mathbb{I}[\mathbf{G}(\boldsymbol{\theta})] = 1\} \quad (2)$$

where  $\mathbb{I} : \mathbb{R}^{n_g} \rightarrow \{0, 1\}$  is the indicator function that allocates a value of 1 if the constraints are satisfied, and 0 otherwise. In this context, nested sampling proceeds by: (i) maintaining a set of live points,  $\mathcal{S}_L := \{\boldsymbol{\theta}^{(1)}, \dots, \boldsymbol{\theta}^{(L)}\}$ ; (ii) drawing proposal points,  $\boldsymbol{\theta}^{(p)}$ , from a uniform prior,  $p(\boldsymbol{\theta})$ , with support provided by a user-defined set,  $\mathcal{K}_\theta$ ; (iii) either accepting or rejecting the proposals if the constraint  $\mathbb{I}[\mathbf{G}(\boldsymbol{\theta}^{(p)})] > \min_{\boldsymbol{\theta} \in \mathcal{S}_L} \mathbb{I}[\mathbf{G}(\boldsymbol{\theta})]$  is satisfied or not; and (iv) if the point is accepted, dropping the previous live set point with minimum likelihood value from the live set and storing it as dead point. This process enables the live

set to progressively concentrate on regions of the space that satisfy constraints as steps (ii)–(iv) are repeated. The search is terminated once all members of the live set ensure the system of inequalities; the final live set then provides an inner approximation to  $\Theta$  with (no less than)  $L$  elements.

The benefits of nested sampling relative to other Monte Carlo approaches lie in efficiency, as inherited through extensions that improve the proposal sampling policy (Speagle, 2020). Since using an indicator function as analogue to the likelihood is unlikely to inherit these accelerations, a preferable analogue is provided by a smooth monotonically decreasing, scalar-valued function with a domain defined by the co-domain of the constraint violation. Refer to Paulen et al. (2020) and Skilling (2006) for more discussion in this direction.

## 3. METHODOLOGY

### 3.1 Multi-Unit Feasible Space Characterization

Our problem setup assumes a set of units,  $\mathcal{N} := \{1, \dots, N\}$ , whose connectivity may be described as a directed acyclic graph (DAG),  $\mathcal{G} := (\mathcal{N}, \mathcal{E})$ , where  $(i, j) \in \mathcal{E}$  defines a directed connection between unit  $i \in \mathcal{N}$  and unit  $j \in \mathcal{N}$ . The connectivity of the DAG may be described equivalently by a non-symmetric adjacency matrix,  $A \in \{0, 1\}^{N \times N}$ , with element  $a_{ij} = 1$  indicating a connection between unit  $i$  and unit  $j$ .

The following data is assumed for each unit  $i \in \mathcal{N}$ :

- A set of in-neighbours which provide inlet streams to unit  $i$ , denoted by  $\mathcal{N}_i^{\text{in}}$ ;
- A set of out-neighbours which receive outlet streams from unit  $i$ , denoted by  $\mathcal{N}_i^{\text{out}}$ ;
- The properties of any inlet stream to unit  $i$  from an in-neighbour  $j \in \mathcal{N}_i^{\text{in}}$ , denoted by  $\mathbf{u}_i^j \in \mathbb{R}^{n_{u_{ij}}}$ ;<sup>1</sup>
- The properties of any outlet stream from unit  $i$  connected to an out-neighbour  $k \in \mathcal{N}_i^{\text{out}}$ , denoted by  $\mathbf{y}_i^k \in \mathbb{R}^{n_{y_{ik}}}$ ;
- The relations between the stream properties at the outlet of unit  $i$  and its inlet properties:

$$\mathbf{y}_i = \mathbf{F}_i(\mathbf{v}_i, \mathbf{u}_i) \quad (3)$$

where  $\mathbf{v}_i \in \mathbb{R}^{n_{v_i}}$  are process variables local to unit  $i$ , and  $\mathbf{u}_i := (\mathbf{u}_i^j)_{j \in \mathcal{N}_i^{\text{in}}} \in \mathbb{R}^{n_{u_i}}$  denotes the concatenation of all inlet stream properties to unit  $i$ ;<sup>2</sup>

- The relations between the stream properties at the outlet of unit  $i$  to the properties at the inlet of a connected downstream unit  $k \in \mathcal{N}_i^{\text{out}}$ :

$$\mathbf{u}_k^i = \mathbf{C}_k^i(\mathbf{y}_i); \quad (4)$$

- Any inequality constraints to be satisfied by the process variables local to unit  $i$ :

$$\mathbf{G}_i(\mathbf{v}_i, \mathbf{u}_i) := \mathbf{g}_i(\mathbf{v}_i, \mathbf{u}_i, \mathbf{y}_i) \leq \mathbf{0}. \quad (5)$$

<sup>1</sup> External inlet streams to any of the units may also be included in the problem statement, but they are omitted here for notational simplicity.

<sup>2</sup> The mappings  $\mathbf{F}_i$  need not be given in closed-form but could be implicitly defined by a set of algebraic or differential equations or even black-box functions such as a process simulator. It is also worth highlighting that these mappings assume nominal descriptions of uncertain process parameters, such as reaction kinetic parameters.

The challenge that is posed by multi-unit feasibility characterization is to identify the values of  $\mathbf{v} := (\mathbf{v}_i)_{i \in \mathcal{N}} \in \mathbb{R}^{n_v}$  that satisfy all of the constraints imposed on all of the local process variables. Formally, such a multi-unit space may be defined as:

$$\mathbb{V} := \left\{ \mathbf{v} \in \mathcal{K}_v \left| \begin{array}{l} \forall i \in \mathcal{N}, \exists \mathbf{u}_i \in \mathbb{R}^{n_{u_i}} : \\ \mathbf{0} \geq \mathbf{G}_i(\mathbf{v}_i, \mathbf{u}_i) \\ \mathbf{u}_k^i = \mathbf{C}_k^i(\mathbf{F}_i(\mathbf{v}_i, \mathbf{u}_i)), \forall k \in \mathcal{N}_i^{\text{out}} \end{array} \right. \right\} \quad (6)$$

where  $\mathcal{K}_v := \prod_{i \in \mathcal{N}} \mathcal{K}_{v_i} \subset \mathbb{R}^{n_v}$  describes the search space of local unit process variables  $\mathbf{v}$ , which is typically available from preexisting experimental campaigns<sup>3</sup>.

Notice that recursive substitution of the unit inlet properties  $\mathbf{u}_i$  with their upstream dependencies  $\mathbf{C}_k^i(\mathbf{F}_i(\mathbf{v}_i, \mathbf{u}_i))$ ,  $k \in \mathcal{N}_i^{\text{out}}$  in the constraint expressions  $\mathbf{G}_i(\mathbf{v}_i, \mathbf{u}_i) \leq \mathbf{0}$  would lead to an equivalent formulation of (6) as:

$$\mathbb{V} := \{ \mathbf{v} \in \mathcal{K}_v \mid \mathbf{G}(\mathbf{v}) \leq \mathbf{0} \} \quad (7)$$

Then similar to (1), a sampling-based algorithm such as nested sampling could be applied to compute a set of samples that satisfy all of the process constraints (5) alongside the process model equations (3)–(4). We refer to this as the simultaneous approach. Clearly, the combined dimensionality  $n_v = \sum_{i \in \mathcal{N}} n_{v_i}$  must be small enough for problem (7) to remain tractable using sampling. This is because the expense will increase with the volume of the search space, which is exponential in the dimension size  $n_v$ . To overcome these scalability challenges, we propose to leverage process structure in a manner amenable to use of any adaptive sampling approach.

### 3.2 Decomposition Approach

We explore methodology to decompose the multi-unit identification into separate unit-wise subproblems, to be solved incrementally. The result of this incremental identification determines a tight enclosure  $\bar{\mathbb{V}} \supseteq \mathbb{V}$  of the multi-unit feasible region in (6). As such, decomposition effectively provides a space reduction strategy, as the joint multi-unit feasible region may be reconstructed from  $\bar{\mathbb{V}}$  thereafter. By decomposing the problem into a series of subproblems with lower dimensionality, therefore, we hypothesize that the overall efficiency of multi-unit identification will be improved.

*Local Feasible Space Subproblems* The problem structure described in Section 3.1 admits a decomposition because the inequality constraints (5) are imposed on each unit in terms of their local unit variables only. This leads to a block diagonal structure in the biadjacency matrix of a variable-constraint bipartite network representing the simultaneous problem (Daoutidis et al., 2019).

For each unit  $i \in \mathcal{N}$ , we consider an extended local feasible space (FS) that jointly describes their local process variables  $\mathbf{v}_i$  and their inlet stream properties  $\mathbf{u}_i$ , so that for operation under any pair  $(\mathbf{v}_i, \mathbf{u}_i) \in \mathbb{V}U_i$ , (i) the local constraints  $\mathbf{G}_i(\mathbf{v}_i, \mathbf{u}_i) \leq \mathbf{0}$  are satisfied, and (ii) for all out-neighbours  $k \in \mathcal{N}_i^{\text{out}}$ , there exists a setting  $(\mathbf{v}_k, \mathbf{u}_k)$  under

which the local constraints  $\mathbf{G}_k(\mathbf{v}_k, \mathbf{u}_k) \leq \mathbf{0}$  are satisfied. The extended local FS is defined as follows:

$$\bar{\mathbb{V}}U_i := \left\{ (\mathbf{v}_i, \mathbf{u}_i) \in \mathcal{K}_{vu_i} \left| \begin{array}{l} \mathbf{0} \geq \mathbf{G}_i(\mathbf{v}_i, \mathbf{u}_i) \\ \forall k \in \mathcal{N}_i^{\text{out}}, \exists (\mathbf{v}_k, \mathbf{u}_k) \in \bar{\mathbb{V}}U_k : \\ \mathbf{u}_k^i = \mathbf{C}_k^i(\mathbf{F}_i(\mathbf{v}_i, \mathbf{u}_i)) \end{array} \right. \right\} \quad (8)$$

with  $\mathcal{K}_{vu_i} := \mathcal{K}_{v_i} \times \mathcal{K}_{u_i}$ , and  $\mathcal{K}_{u_i}$  is the search space of the inlet stream to unit  $i$ . Although one may assume a priori knowledge about  $\mathcal{K}_{v_i}$ , this may not be the case for  $\mathcal{K}_{u_i}$ . Herein, we estimate  $\mathcal{K}_{u_i}$  via a two-step approach, first gathering realizations  $\mathbf{u}_i \in \mathcal{K}_{v_i}$  for each unit through simulations of the multi-unit process under different scenarios of  $\mathbf{v} \in \mathcal{K}_v$  generated through a space filling design, then forming an outer-approximation (e.g., a box enclosure) to the realizations gathered.

It is important to note that the set  $\bar{\mathbb{V}}U_i$  yields a superset to the actual FS of unit  $i$ , given by:

$$\mathbb{V}U_i := \left\{ (\mathbf{v}_i, \mathbf{u}_i) \in \mathcal{K}_{vu_i} \left| \begin{array}{l} \mathbf{0} \geq \mathbf{G}_i(\mathbf{v}_i, \mathbf{u}_i) \\ \forall k \in \mathcal{N}_i^{\text{out}}, \exists (\mathbf{v}_k, \mathbf{u}_k) \in \mathbb{V}U_k : \\ \mathbf{u}_k^i = \mathbf{C}_k^i(\mathbf{F}_i(\mathbf{v}_i, \mathbf{u}_i)) \\ \forall j \in \mathcal{N}_i^{\text{in}}, \exists (\mathbf{v}_j, \mathbf{u}_j) \in \mathbb{V}U_j : \\ \mathbf{u}_j^i = \mathbf{C}_j^i(\mathbf{F}_j(\mathbf{v}_j, \mathbf{u}_j)) \end{array} \right. \right\}. \quad (9)$$

This is because the definition of  $\bar{\mathbb{V}}U_i$  in (8) omits further restrictions imposed by in-neighbors  $j \in \mathcal{N}_i^{\text{in}}$  on the inlet stream properties  $\mathbf{u}_i^j$ . As a result, the projections of the sets  $\bar{\mathbb{V}}U_i$  onto the subspace of local process variables, given by:

$$\bar{\mathbb{V}}_i := \{ \mathbf{v}_i \in \mathcal{K}_{v_i} \mid \exists \mathbf{u}_i \in \mathcal{K}_{u_i} : (\mathbf{v}_i, \mathbf{u}_i) \in \bar{\mathbb{V}}U_i \} \quad (10)$$

describe a superset to the projected multi-unit FS,  $\bar{\mathbb{V}}_i \supseteq \mathbb{V}_i$ , and one has:

$$\bar{\mathbb{V}} := \prod_{i \in \mathcal{N}} \bar{\mathbb{V}}_i \supseteq \mathbb{V}. \quad (11)$$

*Back-Propagation Policy and Surrogate Constraints* The recursive definition of extended local FS in (8) imposes back-propagation of  $\bar{\mathbb{V}}U_i$  from downstream to upstream units as the natural evaluation order. Formally, we can define a partial order among units such that  $i \prec k$  whenever  $k \in \mathcal{N}_i^{\text{out}}$ , and we assume here, without the loss of generality, that  $1 \prec 2 \prec \dots \prec N$ .

Such ordering of the units is straightforward for small acyclic process networks. For larger networks, this task could be automated, e.g., using the Coffman-Graham algorithm, which is commonly applied to job-shop scheduling problems under precedence constraints between tasks (Coffman and Graham, 1972).<sup>4</sup>

An observation that provides intuition for the use of back-propagation is that the leaf nodes in a DAG, such as  $N$ , are the only nodes from which one can initially solve a subproblem. This is because leaf nodes have no out-neighbors and, therefore, no complicating constraints:

$$\bar{\mathbb{V}}U_N = \{ (\mathbf{v}_N, \mathbf{u}_N) \in \mathcal{K}_{vu_N} \mid \mathbf{0} \geq \mathbf{G}_N(\mathbf{v}_N, \mathbf{u}_N) \} \quad (12)$$

<sup>3</sup> As indicated by the notation, the search space is synonymous with the knowledge space common to design space problems in pharmaceutical manufacturing.

<sup>4</sup> For the Coffman-Graham algorithm to be applied appropriately in a back-propagation context, it should be applied to the transpose  $A^T$  of the DAG's adjacency matrix. It is worth highlighting that the Coffman-Graham algorithm could also identify an appropriate assignment and sequencing of subproblems for parallel computation.

For a unit  $i$  other than a leaf node, characterization of the extended local FS,  $\overline{\mathbb{V}}U_i$ , is challenged by the fact that the extended local FS of any of its out-neighbours  $k \in \mathcal{N}_i^{\text{out}}$ ,  $\overline{\mathbb{V}}U_k$ , is not known in closed form. With a sampling-based algorithm such as nested sampling, one may only determine an inner-approximation of  $\overline{\mathbb{V}}U_k$  as a finite collection of feasible settings  $(\mathbf{v}_k, \mathbf{u}_k)$ . Our approach to making  $\overline{\mathbb{V}}U_i$  in (8) compliant with the generic setup in (1), entails the training of surrogate constraint functions  $\overline{\mathbf{G}}_k : \mathbb{R}^{n_{v_k}} \times \mathbb{R}^{n_{u_k}} \rightarrow \mathbb{R}$  such that:

$$\overline{\mathbb{V}}U_k \approx \{(\mathbf{v}_k, \mathbf{u}_k) \in \mathcal{K}_{vu_k} \mid \mathbf{0} \geq \overline{\mathbf{G}}_k(\mathbf{v}_k, \mathbf{u}_k)\}. \quad (13)$$

This then allows approximating the extended local FS of unit  $i$  as:

$$\overline{\mathbb{V}}U_i \approx \left\{ (\mathbf{v}_i, \mathbf{u}_i) \in \mathcal{K}_{vu_i} \left| \begin{array}{l} \mathbf{0} \geq \mathbf{G}_i(\mathbf{v}_i, \mathbf{u}_i) \\ \forall k \in \mathcal{N}_i^{\text{out}}, \\ \mathbf{0} \geq \min_{(\mathbf{v}_k, \mathbf{u}_k) \in \mathcal{K}_{vu_k}} \overline{\mathbf{G}}_k(\mathbf{v}_k, \mathbf{u}_k) \\ \text{s.t. } \mathbf{u}_k^i = \mathbf{C}_k^i(\mathbf{F}_i(\mathbf{v}_i, \mathbf{u}_i)) \end{array} \right. \right\}, \quad (14)$$

which can now be sampled via the solution of auxiliary optimization problems.

*Final Reconstruction* After back-propagating the extended local FS,  $\overline{\mathbb{V}}U_i$ , through each unit  $i \in \mathcal{N}$  of the acyclic process network, it is immediate to determine an inner-approximation of  $\overline{\mathbb{V}}_i$  in (10) by projection. The multi-unit FS,  $\mathbb{V}$  is defined as in (6), yet with the notable difference that the original search space  $\mathcal{K}_v$  can now be replaced with the tighter Cartesian product set  $\overline{\mathbb{V}}$ :

$$\mathbb{V} = \left\{ \mathbf{v} \in \overline{\mathbb{V}} \left| \begin{array}{l} \forall i \in \mathcal{N}, \exists \mathbf{u}_i \in \mathbb{R}^{n_{u_i}} : \\ \mathbf{0} \geq \mathbf{G}_i(\mathbf{v}_i, \mathbf{u}_i) \\ \mathbf{u}_k^i = \mathbf{C}_k^i(\mathbf{F}_i(\mathbf{v}_i, \mathbf{u}_i)), \forall k \in \mathcal{N}_i^{\text{out}} \end{array} \right. \right\} \quad (15)$$

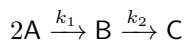
Our main hypothesis is that reconstructing  $\mathbb{V}$  from  $\overline{\mathbb{V}}$  rather than  $\mathcal{K}_v$  might significantly reduce the number of process model evaluations. In principle, one could apply nested sampling to determine (15). Instead, it is proposed to evaluate different points in  $\overline{\mathbb{V}}$  by sampling a uniform random distribution with support provided by the discrete sets returned by nested sampling in decomposition,  $\overline{\mathbb{V}}_i \forall i \in \mathcal{N}$ , and evaluating them under the process model until a sufficient number of points characterize the multi-unit feasible region.

Finally, the recursive procedure of local FS characterization and surrogate constraint learning, followed by the joint FS identification, is summarized by Algorithm 1.

## 4. CASE STUDY

### 4.1 Problem Definition

We demonstrate the decomposition approach on a batch chemical reactor network that consists of two batch reactors connected in series (Figure 1). The reaction mechanism characterizing the reactors is the same:



where component B is the desired product with modified kinetics compared to Kucherenko et al. (2020).

The reactor dynamics are ODEs that describe the evolution of component molar concentrations in continuous time. The system adheres to Arrhenius kinetics:

---

### Algorithm 1. Decomposition of feasibility characterization in acyclic multi-unit processes

---

**Require:** DAG representative of unit connectivity,  $\mathcal{G} = (\mathcal{N}, \mathcal{E})$ , with set of units  $\mathcal{N}$  such that  $1 \prec 2 \prec \dots \prec N$

**1.** Estimate the search space of inlet variables  $\mathcal{K}_{u_i}$  in each unit  $i \in \mathcal{N}$  through simulating the multi-unit network using different settings of  $\mathbf{v} \in \mathcal{K}_v$  generated from space filling design such as Sobol' sequence

**for all**  $i \in [N, N-1, \dots, 1]$  **do**

**2a.** Determine an inner-approximation of  $\overline{\mathbb{V}}U_i$  as defined in (14) using surrogate constraints for each out-neighbour unit  $k \in \mathcal{N}_i^{\text{out}}$

**2b.** Project  $\overline{\mathbb{V}}U_i$  to determine an inner-approximation of  $\overline{\mathbb{V}}_i$  as in (10) and store in memory

**2c.** Learn a surrogate constraint  $\overline{\mathbf{G}}_i$  of  $\overline{\mathbb{V}}U_i$  as defined in (13)

**end for**

**3.** Sample the multi-unit FS  $\mathbb{V}$  in (15) with a uniform prior defined on the Cartesian product  $\overline{\mathbb{V}} := \prod_{i \in \mathcal{N}} \overline{\mathbb{V}}_i$

**Output:** Inner-approximation of multi-unit FS,  $\mathbb{V}$

---

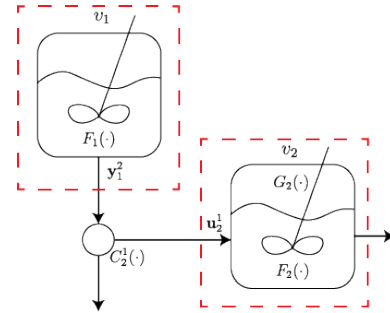


Fig. 1. Case study illustration. A reactor network consisting of two batch process systems in series. Red boxes indicate the nodes of a process representative DAG.

Parameter	Reaction 1	Reaction 2
$k_r^\circ$ ( $\text{m}^3 \text{ kmol}^{-1} \text{ min}^{-1}$ )	$6.66 \times 10^{-3}$	1.03
$E_r$ ( $\text{kJ mol}^{-1}$ )	2.52	5.00

Table 1. Arrhenius kinetic parameters used in case study

$$k_r(T) = k_r^\circ \exp\left(-\frac{E_r}{RT}\right)$$

where  $T$  is the reaction temperature;  $k_r$ , the temperature-dependent rate constant of reaction step  $r \in \{1, 2\}$ ;  $k_r^\circ$ , the pre-exponential factor;  $E_r$ , the activation energy; and  $R$  denotes the ideal gas constant. The kinetic parameters are detailed by Table 1. The volume of both reactors is assumed  $V = 1 \text{ m}^3$ . Each ODE system is given by:

$$\dot{c}_{A,j}(t) = -2k_1(T_j) c_{A,j}(t)^2 \quad (16)$$

$$\dot{c}_{B,j}(t) = k_1(T_j) c_{A,j}(t)^2 - k_2(T_j) c_{B,j}(t) \quad (17)$$

$$\dot{c}_{C,j}(t) = k_2(T_j) c_{B,j}(t) \quad (18)$$

where  $c_{i,j}(t)$  ( $\text{kmol m}^{-3}$ ) describes the molar concentration of component  $i$  in reactor  $j$ ; and  $T_j$ , the temperature

in reactor  $j$ . Each reactor is operated over a time horizon,  $t \in [0, \tau_j]$ , where  $\tau_j$  is the batch time. The initial concentration of the first reactor is  $\mathbf{c}_1(0) = [2 \ 0 \ 0]^\top$ , whereas the initial concentration of the second reactor is  $\mathbf{c}_2(0) = [c_{A,1}(\tau_1) \ c_{B,1}(\tau_1) \ 0]^\top$ . Here, we assume that the initial concentration of the second reactor is equal to the composition present in the first reactor at the batch end-point, subject to a separation step to completely remove the (inert) component C. This operation is considered perfect and, therefore, is excluded from the FS identification.

The process parameters of interest in the FS characterization are the temperature and batch time of both reactors, such that  $\mathbf{v}_j = [T_j \ \tau_j]^\top$ . An inequality constraint is imposed to ensure the molar purity of component B at the end of operating the second batch reactor:

$$\frac{c_{B,2}(\tau_2)}{c_{A,2}(\tau_2) + c_{B,2}(\tau_2) + c_{C,2}(\tau_2)} \geq b$$

with a minimal purity target of  $b = 0.82$ . The search spaces  $\mathcal{K}_{v_1}$  and  $\mathcal{K}_{v_2}$  are defined such that  $\tau_j \in [250, 800]$  (min) and  $T_j \in [250, 1000]$  (K).

#### 4.2 Implementation Details

The nested sampling and decomposition algorithms are fully implemented within Python 3.10.12. All runs of the nested sampling algorithm, including both the simultaneous and incremental FS identifications, consider 4000 live points and draw 50 candidate replacement points at each iteration. The search is terminated when all the live points satisfy the imposed constraints. The nested sampling algorithm is provided by the DEUS package<sup>5</sup>. Additionally, the ODE systems definitive of reactor dynamics are all solved with the same numerical integration scheme, specifically a Tsitouras' 5/4 Runge Kutta method (Tsitouras, 2011) implemented within DIFFRAX (Kidger, 2022).

Specific to the decomposition method, we parameterise the surrogate constraints  $\mathbf{G}_k(\mathbf{v}_k, \mathbf{u}_k), \forall k \in \mathcal{N}_i^{\text{out}}$ , constituent of each FS subproblem  $\overline{\mathbb{V}}_i$ , via support vector machine (SVM) classifiers with radial basis function (RBF) kernel. The hyperparameters are the regularization weight controlling the softness of the margin, and the shape parameter of the RBF kernel. They are selected through 10-fold cross validation and grid search, which leverages the in-silico data generated in identification of the extended local FS,  $\overline{\mathbb{V}}_k$ . This framework is implemented via the scikit-learn 1.10.1 package. The auxiliary optimization problems are solved as box-constrained nonlinear programs using the Limited memory Broyden-Fletcher-Goldfarb-Shanno-B (LBFGSB) algorithm implemented in JAXopt 0.8.2. In the forward pass to initialise  $\mathcal{K}_{u_2}$ , we utilize 4096 Sobol samples of  $\mathbf{v} \in \mathcal{K}_v$ , and then define  $\mathcal{K}_{u_2}$  as a box enclosure to the data generated. Specifically, we magnify the range of the data in each dimension by a factor of 1.05.

#### 4.3 Results and Discussion

The problem decomposes unit-wise via the proposed approach into two subproblems, with  $1 \prec 2$ . For reactor 2, the extended FS  $\overline{\mathbb{V}}_2$  is constituted by four variables  $(\mathbf{v}_2, \mathbf{u}_2^1) \in \mathbb{R}^2 \times \mathbb{R}^2$ , with  $\mathbf{u}_2^1$  indicating the initial molar

<sup>5</sup> The package is available at <https://github.com/omega-icl/deus>

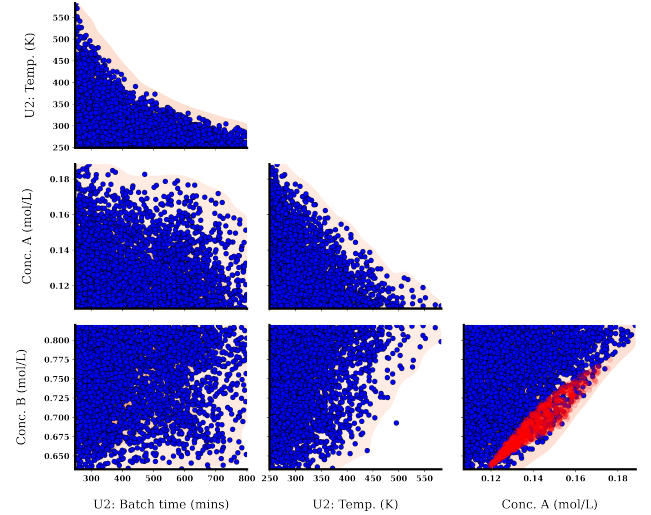


Fig. 2. Coupling between the decomposed feasible spaces. The plot indicates the live set of reactor 2 (blue scatter), the inlets to reactor 2 as a result of operating reactor 1 according to its extended feasible space (lightly transparent, red scatter), and a kernel density estimate to the region deemed to satisfy constraints by the SVM classifier (light red shaded region).

concentration of components A and B at the start of the second batch, which is identical to that present at the end of the first batch. An inner-approximation with 4000 samples determined by nested sampling (live set) is shown in Figure 2 (dark blue point). Next, an SVM classifier is trained to couple the extended FS  $\overline{\mathbb{V}}_2$  to that of reactor 1 upstream. The classifier selected via the cross-validation framework had an average validation accuracy of 99.7%. The region of the extended search space characterized as feasible by the SVM classifier is illustrated in light red on Figure 2.

Since the initial concentration  $\mathbf{c}_1(0)$  in the first batch is set, the extended FS  $\overline{\mathbb{V}}_1$  of reactor 1 is constituted by two variables  $\mathbf{v}_1 \in \mathbb{R}^2$  only. After computing an inner-approximation of  $\overline{\mathbb{V}}_1$  with 4000 samples by nested sampling, the resultant mapping  $\mathbf{u}_2^1 = C_2^1(F_1^2(\mathbf{v}_1))$  is superimposed to Figure 2 via the (lightly transparent) red scatter points.

The final step entails reconstructing the multi-unit FS as described in Section 3.2.3 according to a uniform prior on the discrete inner approximation to  $\overline{\mathbb{V}}_1 \times \overline{\mathbb{V}}_2$  as provided by the initial decomposition. The final result of the decomposition approach is detailed on Figure 3.

From comparison of the figures it is clear that the volume of the multi-unit FS has been well recovered, indicating that the procedure coupling the spaces is effective. This is highlighted through comparisons of the projected set  $\overline{\mathbb{V}}_2$  from the live set of reactor 2, as visualized in Figure 2, and the actual set  $\mathbb{V}_2$  plotted in Figure 3. Figure 2 additionally demonstrates that the classifier parameterizes the FS of reactor 2 as a superset of the joint multi-unit FS projection. This is because the extended FS  $\overline{\mathbb{V}}_2$  upon which it is trained is also a superset to the multi-unit FS projection.

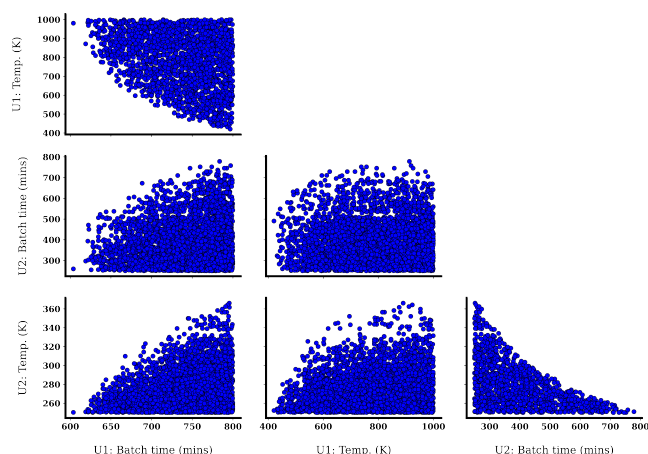


Fig. 3. The multi-unit feasible space identified through decomposition.

Interestingly, the decomposition method requires approximately half (54%) the total number of function evaluations in comparison to the method without decomposition (i.e. simultaneously with a uniform prior on  $\mathcal{K}_{v_1} \times \mathcal{K}_{v_2}$ ), where we regard a function evaluation as a numerical simulation of one batch reactor. While case dependent, this result is encouraging insofar as the FS subproblem for reactor 2 in the decomposition method has the same dimensionality as the multi-unit FS itself. A likely explanation for this behavior is that the extended search space of reactor 2,  $\mathcal{K}_{v_{u_2}}$  has a smaller volume than that of the multi-unit search space  $\mathcal{K}_{v_1} \times \mathcal{K}_{v_2}$ , resulting in improved acceptance rates in nested sampling iterations.

## 5. CONCLUSIONS

A decomposition approach to sampling-based feasibility in acyclic multi-unit processes has been presented. The approach back-propagates unit-level FS subproblems that are coupled via a constraint learning strategy to account for restrictions imposed on the downstream units. The joint FS is then reconstructed from the unit-level projections generated, which define a tighter prior than the search space. We demonstrated that the decomposition can enable more efficient FS characterization compared to directly sampling from the search space, with the benefit of reduced model evaluations in the case study. The key assumption of the work is that the process network can be represented as a DAG, which requires subgraphs with recycle structures to be identified simultaneously at present. In future, we will provide methodology to consider recycles unit-wise, extend to the probabilistic FS, and explore means to improve efficiency further.

## REFERENCES

Coffman, E.G. and Graham, R.L. (1972). Optimal scheduling for two-processor systems. *Acta Informatica*, 1, 200–213.

Daoutidis, P., Tang, W., and Allman, A. (2019). Decomposition of control and optimization problems by network structure: Concepts, methods, and inspirations from biology. *AIChE Journal*, 65(10), e16708.

Geremia, M., Bezzo, F., and Ierapetritou, M.G. (2024). Design space determination of pharmaceutical pro-

cesses: Effects of control strategies and uncertainty. *European Journal of Pharmaceutics & Biopharmaceutics*, 194, 159–169.

Harwood, S.M. and Barton, P.I. (2017). How to solve a design centering problem. *Mathematical Methods of Operations Research*, 86, 215–254.

Kidger, P. (2022). On neural differential equations. *arXiv preprint arXiv:2202.02435*.

Kucherenko, S., Giamalakis, D., Shah, N., and García-Muñoz, S. (2020). Computationally efficient identification of probabilistic design spaces through application of metamodeling and adaptive sampling. *Computers & Chemical Engineering*, 132, 106608.

Kudva, A., Tang, W.T., and Paulson, J.A. (2024). Robust Bayesian optimization for flexibility analysis of expensive simulation-based models with rigorous uncertainty bounds. *Computers & Chemical Engineering*, 181, 108515.

Kusumo, K.P., Gomoescu, L., Paulen, R., García Muñoz, S., Pantelides, C.C., Shah, N., and Chachuat, B. (2019). Bayesian approach to probabilistic design space characterization: A nested sampling strategy. *Industrial & Engineering Chemistry Research*, 59(6), 2396–2408.

Paulen, R., Gomoescu, L., and Chachuat, B. (2020). Nested sampling approach to set-membership estimation. *IFAC-PapersOnLine*, 53(2), 7228–7233.

Samsatli, N., Papageorgiou, L., and Shah, N. (1999). Batch process design and operation using operational envelopes. *Computers & Chemical Engineering*, 23, S887–S890.

Skilling, J. (2006). Nested sampling for general Bayesian computation. *Bayesian Analysis*, 1(4), 833–859.

Speagle, J.S. (2020). DYNESTY: a dynamic nested sampling package for estimating Bayesian posteriors and evidences. *Monthly Notices of the Royal Astronomical Society*, 493(3), 3132–3158.

Swaney, R.E. and Grossmann, I.E. (1985). An index for operational flexibility in chemical process design. Part I: Formulation and theory. *AIChE Journal*, 31(4), 621–630.

Tsitouras, C. (2011). Runge–kutta pairs of order 5 (4) satisfying only the first column simplifying assumption. *Computers & Mathematics with Applications*, 62(2), 770–775.

von Stosch, M., Schenkendorf, R., Geldhof, G., Varsakelis, C., Mariti, M., Dessoy, S., Vandercammen, A., Pysik, A., and Sanders, M. (2020). Working within the design space: do our static process characterization methods suffice? *Pharmaceutics*, 12(6), 562.

Yu, L.X., Amidon, G., Khan, M.A., Hoag, S.W., Polli, J., Raju, G., and Woodcock, J. (2014). Understanding pharmaceutical quality by design. *The AAPS Journal*, 16, 771–783.

Zhao, F., Grossmann, I.E., García-Muñoz, S., and Stamatias, S.D. (2022a). Design space description through adaptive sampling and symbolic computation. *AIChE Journal*, 68(5), e17604.

Zhao, F., Ochoa, M.P., Grossmann, I.E., García-Muñoz, S., and Stamatias, S.D. (2022b). Novel formulations of flexibility index and design centering for design space definition. *Computers & Chemical Engineering*, 166, 107969.